

Computational Fluid Dynamics: Assignment 1.3

Student : Toby van Gastelen (5373123)
TU Delft

I. METHOD OF MANUFACTURED SOLUTIONS

A. Problem statement

Let us start by considering the boundary value problem (BVP)

$$\begin{aligned} \phi_{,1}(x) - \epsilon \phi_{,11} &= q(x), \quad x \in \Omega \\ \phi(0) &= a, \quad \phi(1) = b \end{aligned} \quad (1)$$

with $\Omega = [0, 1]$, $0 < \epsilon \ll 1$, and $a, b \in \mathbb{R}$. We will treat this problem numerically using cell-centered finite-volumes.

B. Convergence of the numerical simulation

To test the convergence of the numerical solution for $q = 0$ and $\epsilon = 0.01$ we first note that the exact solution of BVP (1) is given by

$$\phi(x) = a + (b - a) \frac{e^{\frac{x-1}{\epsilon}} - e^{-1/\epsilon}}{1 - e^{-1/\epsilon}}. \quad (2)$$

The numerical implementation of the cell-centered finite volume discretization along with the exact solution were given in the provided MATLAB scripts on Brightspace. To do the analysis I ported the numerical solver over to Python. For the numerical implementation we use the central approximation for both convective and diffusive fluxes. The derivation of the discretization is not included here, as this was not asked in the assignment. To test the convergence of the solution we use the error measure $\|e\|_{l_2}$ defined as:

$$\|e\|_{l_2} = J^{-\frac{1}{2}} \sqrt{\sum_{j=1}^J (\phi(x_j) - \phi_j)^2}, \quad (3)$$

where J is the number of finite volumes and ϕ_j the approximation of $\phi(x)$ at point x_j . Another important thing is that we employ a uniform mesh with cells of size h . To confirm that the numerical solution converges with error $\|e\|_{l_2} = \mathcal{O}(h^2)$ we carry out a set of numerical simulations with different values for h , with $a = 0$ and $b = 1$, and evaluate $\|e\|_{l_2}$. Using the exact solution, provided in (2), we can easily confirm the convergence behavior by fitting to the relation

$$\|e\|_{l_2} \approx Ch^p, \quad (4)$$

where C and p are the fitted parameters. For the fitting procedure we use the non-linear least-squares method provided in the [SciPy](#) package. The results are depicted in figure 1. Here we find a p -value of 2.0298, which closely matches the expected behavior of $\mathcal{O}(h^2)$.

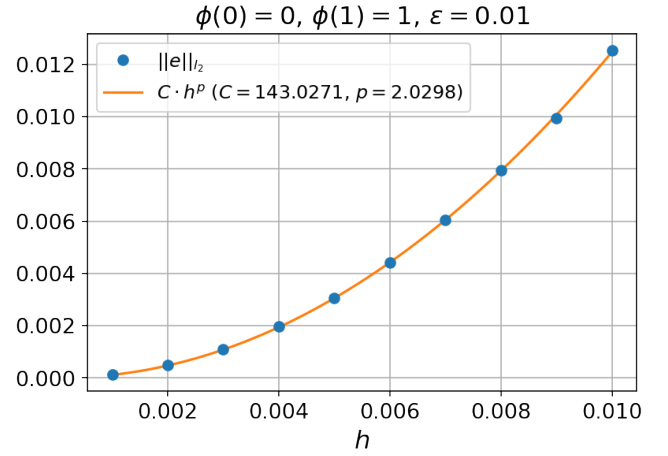


Figure 1: Non-linear least-squares fit of the convergence behavior of the error $\|e\|_{l_2}$, for BVP (1), as a function of cell size h for a uniform mesh and $q(x) = 0$.

C. Manufactured solution

Let us now consider the manufactured solution $\phi_{\text{man}}(x)$ given by

$$\phi_{\text{man}}(x) = \alpha \cos\left(\frac{1}{2}\pi x\right) + \beta(1 - e^x). \quad (5)$$

To make this solution compatible with the boundary conditions we must have that

$$\phi_{\text{man}}(0) = \alpha = a \quad (6)$$

and

$$\phi_{\text{man}}(1) = \beta(1 - e) = b \rightarrow \beta = \frac{b}{1 - e}. \quad (7)$$

Now that we know the coefficients α and β we can find the function $q(x)$ for which $\phi_{\text{man}}(x)$ is a solution to BVP 1. This can simply be done by evaluating the left-hand side of BVP (1), replacing $\phi(x)$ by $\phi_{\text{man}}(x)$. This gives:

$$\begin{aligned} &\phi_{\text{man},1}(x) - \epsilon \phi_{\text{man},11} \\ &= -\frac{\pi\alpha}{2} \sin\left(\frac{\pi}{2}x\right) - \beta e^x - \epsilon \left(-\frac{\pi^2\alpha}{4} \cos\left(\frac{\pi}{2}x\right) - \beta e^x\right) \\ &= q(x). \end{aligned} \quad (8)$$

D. Convergence for the manufactured solution

Let us first reuse our code for the manufactured solution, *i.e.* we use (8) for $q(x)$ along with $a = 1$, $b = 1.1$, and $\epsilon = 0.01$.

For $h = 0.01$ the obtained numerical solution, as well as ϕ_{man} , are shown in 2.

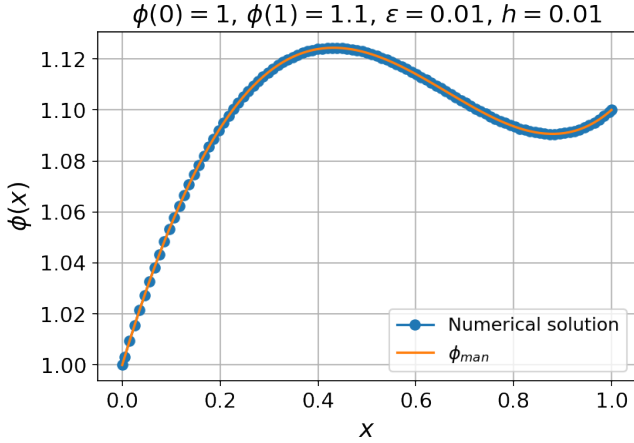


Figure 2: Numerical solution of BVP (1) for $q(x)$ given by (8) as well as the manufactured analytic solution ϕ_{man} .

Let us now reuse the procedure described in section IB and fit the convergence to the relation described by (4) (figure 3). In this case we find $p = 2.0094$ which again confirms the theoretical convergence of behavior of $O(h^2)$ for the error $\|e\|_{l_2}$.

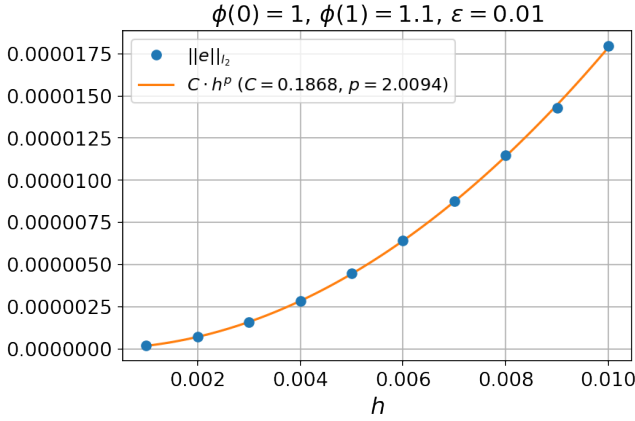


Figure 3: Non-linear least-squares fit of the convergence behavior of the error $\|e\|_{l_2}$, for BVP (1), as a function of cell size h for a uniform mesh and $q(x)$ given by (8).

II. OVERLAPPING GRIDS

A. Problem statement

In this chapter we consider the BVP

$$\begin{aligned} -\phi_{,11} &= q(x), \quad x \in \Omega \\ \phi(0) &= a, \quad \phi(1) = b \end{aligned} \quad (9)$$

with $q(x) = \sin(\pi x)$, $\Omega = [0, 1]$ and $a, b \in \mathbb{R}$. We will again treat this problem numerically using cell-centered finite-volumes, but this time with overlapping grids. During the entirety of this chapter we will set $a = b = 0$ such that we can easily obtain the analytical solution for this BVP as

$$\phi(x) = \frac{1}{\pi^2} \sin(\pi x). \quad (10)$$

This will be useful later when we investigate the convergence of the numerical solution to the analytic solution.

B. Finite-volume discretization

The finite-volume discretization of BVP (9) is treated in this section. To obtain this discretization we first do the following for cell $\Omega_j = [x_{j-\frac{1}{2}}, x_{j+\frac{1}{2}}]$ centered around x_j :

$$\begin{aligned} -\phi_{,11} dx &= q(x) dx \rightarrow \\ \int_{\Omega_j} -\phi_{,11} dx &= \int_{\Omega_j} q(x) dx \xrightarrow{\text{divergence theorem}} \\ -[\phi_{,1}(x_{j+\frac{1}{2}}) - \phi_{,1}(x_{j-\frac{1}{2}})] &= \int_{\Omega_j} q(x) dx \xrightarrow{\text{approximate integral and derivatives}} \\ -\frac{\phi(x_{j+1}) - \phi(x_j)}{h} + \frac{\phi(x_j) - \phi(x_{j-1}))}{h} &= h q(x_j), \end{aligned} \quad (11)$$

where h is the mesh size in the case of a uniform mesh.

Let us now define the overlapping grids as $\Omega_{\text{fine}} = [0, C_e + B_u]$ and $\Omega_{\text{coarse}} = [C_e - B_u, 1]$, where C_e is the center of the overlap and B_u the buffer value which defines how much the grids overlap. To prevent any issues we make sure that $C_e + B_u < 1 = 1$ and $C_e - B_u > 0$. For both grids we employ a uniform mesh, albeit with different mesh sizes $h = |\Omega_{\text{fine}}|/J$ and $H = |\Omega_{\text{coarse}}|/K$, for Ω_{fine} and Ω_{coarse} respectively. $\phi(x)$ is approximated as $\phi_j \approx \phi(x_j)$ and $\phi_k \approx \phi(X_k)$, on Ω_{fine} and Ω_{coarse} respectively. The cell centers on the grids are $\{x_j\}_{j=1,\dots,J}$ for Ω_{fine} and $\{X_k\}_{k=1,\dots,K}$ for Ω_{coarse} . The transfer between the two grids now happens as follows (note that we use slightly different notation as in the assignment, as we change $\Phi(X_k)$ to $\phi(X_k)$):

$$\Omega_{\text{coarse}} \rightarrow \Omega_{\text{fine}} : \phi(x_{J+1}) = \beta_0^c \phi(X_k) + \beta_1^c \phi(X_{k+1}) + O(H^2) \quad (12)$$

for "virtual interior point" $x_{J+1} = x_J + h$ and corresponding k for which $x_{J+1} \in [X_k, X_{k+1}]$, and

$$\Omega_{\text{fine}} \rightarrow \Omega_{\text{coarse}} : \phi(X_0) = \beta_0^f \phi(x_j) + \beta_1^f \phi(x_{j+1}) + O(h^2) \quad (13)$$

for "virtual interior point" $X_0 = X_1 - H$ and corresponding j for which $X_0 \in [x_j, x_{j+1}]$. The coefficients are easily obtained as

$$\begin{aligned} \beta_0^c &= \frac{x_{J+1} - X_k}{H}, \quad x_{J+1} \in [X_k, X_{k+1}] \\ \beta_1^c &= 1 - \beta_0^c \\ \beta_0^f &= \frac{X_0 - x_j}{h}, \quad X_0 \in [x_j, x_{j+1}] \\ \beta_1^f &= 1 - \beta_0^f. \end{aligned} \quad (14)$$

We can now finally write down the discretization in terms of $\{\phi_j\}_{j=1,\dots,J}$, $\{\Phi_k\}_{k=1,\dots,K}$, $q(x)$, h , H , and boundary values a and b :

$$-\frac{\phi_{j+1} - \phi_j}{h} + 2\frac{\phi_j - a}{h} = hq(x_j), \text{ for } j = 1 \quad (15)$$

$$-\frac{\phi_{j+1} - \phi_j}{h} + \frac{\phi_j - \phi_{j-1}}{h} = hq(x_j), \text{ for } j = 2, \dots, J-1 \quad (16)$$

$$-\frac{\beta_0^c \Phi_k + \beta_1^c \Phi_{k+1} - \phi_j}{h} + \frac{\phi_j - \phi_{j-1}}{h} = hq(x_j), \quad (17)$$

for $j = J$ and $x_{j+1} \in [X_k, X_{k+1}]$

$$-\frac{\Phi_{k+1} - \Phi_k}{H} + \frac{\Phi_k - \beta_0^f \phi_j - \beta_1^f \phi_{j+1}}{H} = Hq(x_k), \quad (18)$$

for $k = 1$ and $X_0 \in [x_j, x_{j+1}]$

$$-\frac{\Phi_{k+1} - \Phi_k}{H} + \frac{\Phi_k - \Phi_{k-1}}{H} = Hq(x_k), \text{ for } k = 2, \dots, K-1 \quad (19)$$

$$-2\frac{b - \Phi_k}{H} + \frac{\Phi_k - \Phi_{k-1}}{H} = Hq(x_k), \text{ for } k = K. \quad (20)$$

This can be written as the discretized operator \mathbf{A} acting on the numerical solution $\mathbf{\Phi} = [\phi_1, \phi_2, \dots, \phi_J, \Phi_1, \Phi_2, \dots, \Phi_K]$ such that

$$\mathbf{A}\mathbf{\Phi} = \mathbf{r}. \quad (21)$$

The exact description of \mathbf{A} and \mathbf{r} will be given in section II D.

C. Local truncation error

Let us now find the local truncation error for each of the approximations in section II B, namely (15)-(20). Let us start with treating (15) by letting the discretized operator \mathbf{A} act on $\phi(x_1)$:

$$\begin{aligned} \mathbf{A}\phi(x_1) &= -\frac{\phi(x_2) - \phi(x_1)}{h} + 2\frac{\phi(x_1) - \phi(0)}{h} \xrightarrow{\text{Taylor's formula}} \\ &= 0 \cdot \phi(x_1) + 0 \cdot \phi'(x_1) - \frac{\phi''(x_1)}{2h}(h^2 + \frac{2}{4}h^2) + \frac{O(h^3)}{h} \\ &= -\frac{3h}{4}\phi''(x_1) + O(h^2) \rightarrow \\ \mathbf{A}\phi(x_1) + h\phi''(x_1) &= \frac{h}{4}\phi''(x_1) + O(h^2) \rightarrow \\ \mathbf{A}\phi(x_1) + hq(x_1) &= \mathbf{A}(\phi(x_1) - \phi_1) = \frac{h}{4}\phi''(x_1) + O(h^2) \end{aligned} \quad (22)$$

where $\mathbf{A}(\phi(x_1) - \phi_1)$ is the local truncation error which in this case is of order $O(h)$.

Let us now move onto (16). Here we have

$$\begin{aligned} \mathbf{A}\phi(x_j) &= -\frac{\phi(x_{j+1}) - \phi(x_j)}{h} + \frac{\phi(x_j) - \phi(x_{j-1}))}{h} \xrightarrow{\text{Taylor's formula}} \\ &= 0 \cdot \phi(x_j) + 0 \cdot \phi'(x_j) - \frac{\phi''(x_j)}{2h}(h^2 + h^2) \\ &\quad - \frac{\phi'''(x_j)}{6h}(h^3 - h^3) + \frac{O(h^4)}{h} \\ \mathbf{A}\phi(x_j) + h\phi''(x_j) &= O(h^3) \rightarrow \\ \mathbf{A}(\phi(x_j) - \phi_j) &= O(h^3). \end{aligned} \quad (23)$$

Next, we move to 17:

$$\begin{aligned} \mathbf{A}\phi(x_j) &= -\frac{\beta_0^c \phi(X_k) + \beta_1^c \phi(X_{k+1}) + O(H^2) - \phi(x_j)}{h} \\ &\quad + \frac{\phi(x_j) - \phi(x_{j-1}))}{h} \xrightarrow{\text{Taylor}} \\ &= \frac{1}{h}\phi(x_j)(2 - 1 - \beta_0^c - \beta_1^c) \\ &\quad - \frac{1}{h}\phi'(x_j)(\beta_0^c(h - \beta_1^c H) + \beta_1^c(h + \beta_0^c H) - h) \\ &\quad - \frac{1}{2h}\phi''(x_j)(\beta_0^c(h - \beta_1^c H)^2 + \beta_1^c(h + \beta_0^c H)^2 + h^2) + O(\frac{H^2}{h}) \\ &= 0 \cdot \phi(x_j) + 0 \cdot \phi'(x_j) \\ &\quad + \phi''(x_j)(-h - \frac{H^2}{h}\beta_0^c\beta_1^c) + O(\frac{H^2}{h}) \rightarrow \\ \mathbf{A}(\phi(x_j) - \phi_j) &= (-\frac{H^2}{h}\beta_0^c\beta_1^c)\phi''(x_j) + O(\frac{H^2}{h}). \end{aligned} \quad (24)$$

Now to 18:

$$\begin{aligned} \mathbf{A}\phi(X_1) &= -\frac{\phi(X_2) - \phi(X_1)}{H} \\ &\quad + \frac{\phi(X_1) - \beta_0^f \phi(x_j) - \beta_1^f \phi(x_{j+1}) + O(h^2)}{H} \xrightarrow{\text{Taylor}} \\ &= \frac{1}{H}\phi(X_1)(2 - 1 - \beta_0^f - \beta_1^f) \\ &\quad - \frac{1}{H}\phi'(X_1)(-\beta_0^f(H + \beta_1^f h) - \beta_1^f(H - \beta_0^f h) + H) \\ &\quad - \frac{1}{2H}\phi''(X_1)(\beta_0^f(H + \beta_1^f h)^2 + \beta_1^f(H - \beta_0^f h)^2 + H^2) + O(\frac{h^2}{H}) \\ &= 0 \cdot \phi(X_1) + 0 \cdot \phi'(X_1) \\ &\quad + \phi''(X_1)(-H - \frac{h^2}{H}\beta_0^f\beta_1^f) + O(\frac{h^2}{H}) \rightarrow \\ \mathbf{A}(\phi(X_1) - \Phi_1) &= (-\frac{h^2}{H}\beta_0^f\beta_1^f)\phi''(X_1) + O(\frac{h^2}{H}). \end{aligned} \quad (25)$$

Onto 19:

$$\begin{aligned}
A\phi(X_k) &= -\frac{\phi(X_{k+1}) - \phi(X_k)}{H} + \frac{\phi(X_k) - \phi(X_{k-1}))}{H} \xrightarrow{\text{Taylor's formula}} \\
&= 0 \cdot \phi(X_k) + 0 \cdot \phi'(X_k) - \frac{\phi''(X_k)}{2H}(H^2 + H^2) - \frac{\phi'''(X_k)}{6H}(H^3 - H^3) \\
&\quad + \frac{O(H^4)}{H} \\
A\phi(X_k) + H\phi''(X_k) &= O(H^3) \rightarrow \\
A(\phi(X_k) - \Phi_k) &= O(H^3).
\end{aligned} \tag{26}$$

Finally for 20 we have:

$$\begin{aligned}
A\phi(X_K) &= -2\frac{\phi(1) - \phi(X_K)}{H} + \frac{\phi(X_K) - \phi(X_{K-1}))}{H} \xrightarrow{\text{Taylor's formula}} \\
&= 0 \cdot \phi(X_K) + 0 \cdot \phi'(X_K) - \frac{\phi''(X_K)}{2H}(H^2 + \frac{2}{4}H^2) + \frac{O(H^3)}{H} \\
&= -\frac{3H}{4}\phi''(X_K) + O(H^2) \rightarrow \\
A(\phi(X_K) - \Phi_K) &= \frac{H}{4}\phi''(X_K) + O(H^2).
\end{aligned} \tag{27}$$

D. Transforming the problem to a linear system

Now that we have obtained the truncation errors we will give the exact description of \mathbf{A} and \mathbf{r} as introduced in section II B. For \mathbf{A} we have

$$A = \begin{bmatrix} A_{11} & A_{12} \\ A_{21} & A_{22} \end{bmatrix} \tag{28}$$

with $A_{11} \in \mathbb{R}^{J \times J}$, $A_{12}, A_{21}^T \in \mathbb{R}^{J \times K}$, $A_{22} \in \mathbb{R}^{K \times K}$. Based on our derivations in section II B we get

$$\begin{aligned}
A_{11}^{11} &= \frac{3}{h} \\
A_{11}^{12} &= -\frac{1}{h} \\
r_1 &= hq(x_1) + \frac{2a}{h},
\end{aligned} \tag{29}$$

where the superscript corresponds to the matrix index (row, column). Next, we have

$$\begin{aligned}
A_{11}^{jj} &= \frac{2}{h} \\
A_{11}^{j(j-1)} &= -\frac{1}{h} \\
A_{11}^{j(j+1)} &= -\frac{1}{h} \\
r_j &= hq(x_j)
\end{aligned} \tag{30}$$

for $j = 2, \dots, J-1$. After this we get

$$\begin{aligned}
A_{11}^{JJ} &= \frac{2}{h} \\
A_{11}^{J(j-1)} &= -\frac{1}{h} \\
r_J &= hq(x_J).
\end{aligned} \tag{31}$$

Analogously we find

$$\begin{aligned}
A_{22}^{11} &= \frac{2}{H} \\
A_{22}^{12} &= -\frac{1}{H} \\
r_{J+1} &= Hq(X_1).
\end{aligned} \tag{32}$$

We also find

$$\begin{aligned}
A_{22}^{kk} &= \frac{2}{H} \\
A_{22}^{k(k-1)} &= -\frac{1}{H} \\
A_{22}^{k(k+1)} &= -\frac{1}{H} \\
r_{J+k} &= Hq(x_k)
\end{aligned} \tag{33}$$

for $k = 2, \dots, K-1$. After this we get

$$\begin{aligned}
A_{22}^{KK} &= \frac{3}{H} \\
A_{22}^{K(K-1)} &= -\frac{1}{H} \\
r_{J+K} &= Hq(X_K) + \frac{2b}{H}.
\end{aligned} \tag{34}$$

Finally we find

$$\begin{aligned}
A_{12}^{Jk} &= -\frac{\beta_0^c}{h} \\
A_{12}^{J(k+1)} &= -\frac{\beta_1^c}{h}
\end{aligned} \tag{35}$$

for k corresponding to $x_{J+1} \in [X_k, X_{k+1}]$ and

$$\begin{aligned}
A_{21}^{0j} &= -\frac{\beta_0^f}{H} \\
A_{21}^{0(j+1)} &= -\frac{\beta_1^f}{H}
\end{aligned} \tag{36}$$

for j corresponding to $X_0 \in [x_j, x_{j+1}]$.

The numerical solution $\Phi = [\phi_1, \phi_2, \dots, \phi_J, \Phi_1, \Phi_2, \dots, \Phi_K]$ can now be obtained by solving

$$\mathbf{A}\Phi = \mathbf{r}. \tag{37}$$

E. Numerical simulation results

Now that we have obtained the required equations we carry out a numerical simulation for $a = 0$ and $b = 0$. The result, along with the analytic solution are depicted in figure 4.

F. Mesh refinement

In order to carry out mesh refinements we first will first find the minimal B_u required for exchange of information between

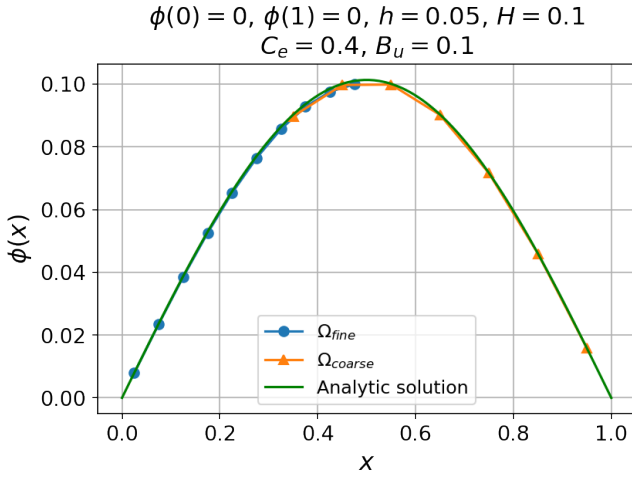


Figure 4: Numerical solution for BVP (9).

Ω_{coarse} and Ω_{fine} . let us first define

$$X_1 - x_J = \frac{h+H}{2} - 2B_u, \quad (38)$$

as for $B_u = 0$ it is easy to see that the overlap between the two regions will be zero. The constraints we have on B_u are that

$$X_1 - x_J = \frac{h+H}{2} - 2B_u \leq \min(h, H) \quad (39)$$

such that for the virtual points x_{J+1} and X_0 the constraints

$$x_{J+1} \geq X_1 \quad (40)$$

and

$$X_0 \leq x_J \quad (41)$$

are satisfied. Replacing \leq by $=$ in (39) and noting that $h = \frac{C_e+B_u}{J}$ and $H = \frac{(1-C_e)+B_u}{K}$ we can write

$$\begin{aligned} \frac{1}{2} \left(\frac{C_e+B_u}{J} + \frac{(1-C_e)+B_u}{K} \right) - 2B_u &= h = \frac{C_e+B_u}{J} \rightarrow \\ B_u \left(-2 - \frac{1}{2J} + \frac{1}{2K} \right) &= \frac{C_e}{2J} + \frac{C_e-1}{2K} \rightarrow \\ B_u^h &= \left(\frac{C_e}{2J} + \frac{C_e-1}{2K} \right) / \left(-2 - \frac{1}{2J} + \frac{1}{2K} \right) \end{aligned} \quad (42)$$

and

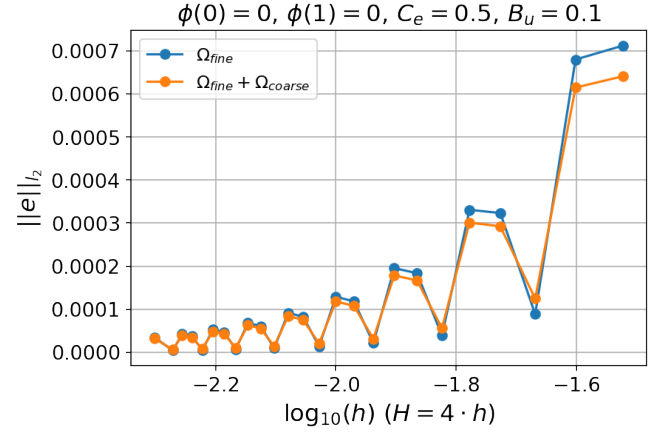
$$\begin{aligned} \frac{1}{2} \left(\frac{C_e+B_u}{J} + \frac{(1-C_e)+B_u}{K} \right) - 2B_u &= H = \frac{(1-C_e)+B_u}{K} \rightarrow \\ B_u \left(-2 + \frac{1}{2J} - \frac{1}{2K} \right) &= -\frac{C_e}{2J} + \frac{1-C_e}{2K} \rightarrow \\ B_u^H &= \left(-\frac{C_e}{2J} + \frac{1-C_e}{2K} \right) / \left(-2 + \frac{1}{2J} - \frac{1}{2K} \right) \end{aligned} \quad (43)$$

accounting for both possibilities in (39). Finally we find that the minimal buffer B_u^{\min} can be written as

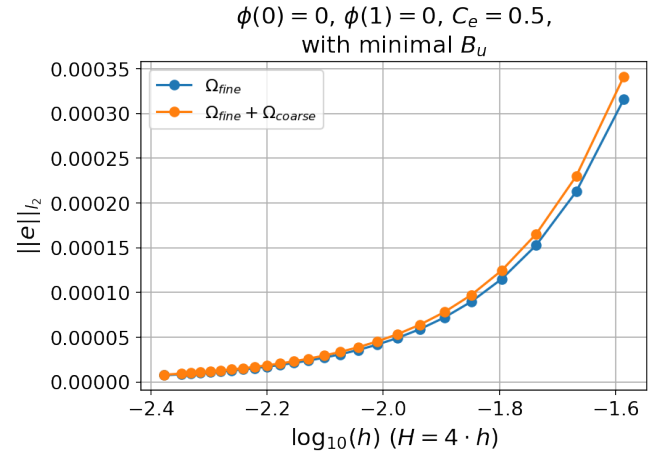
$$B_u^{\min} = \max(B_u^h, B_u^H) \quad (44)$$

depending on J , K , and C_e .

Now we can take a look at a set of numerical experiments. We started by setting $B_u = 0.1$ and varying the cell sizes h and H such that the ratio $H/h = 4$. The results are shown in figure 5. We observe rather large fluctuations in error when compared to the analytic solution found in (10). This is mostly likely caused by the combined effect of the local truncation errors obtained in II C. Next, we take a look at the same variation

Figure 5: $\|e\|_2$ as compared to the analytic solution (10) for a constant B_u evaluated for BVP (9) with $a = b = 0$, varying $h = 4 \cdot H$.

but this time setting $B_u = B_u^{\min}$, which is varied dynamically based on h and H (figure 6). Here we find that error converges much more smoothly.

Figure 6: $\|e\|_2$ as compared to the analytic solution (10) for $B_u = B_u^{\min}$ evaluated for BVP (9) with $a = b = 0$, varying $h = 4 \cdot H$.

Now we carry out a similar experiment, with a constant $B_u = 1$, but we vary the ratio $r = H/h$. The results are shown in figure 7. We now find, what seems to be, a minimum in error for a particular value of r , after which the error solely increases. This likely due to the $O(\frac{H^2}{h})$ error (section II C), which blows

up as r increases. Finally, we repeat this experiment again, but

ratio r .

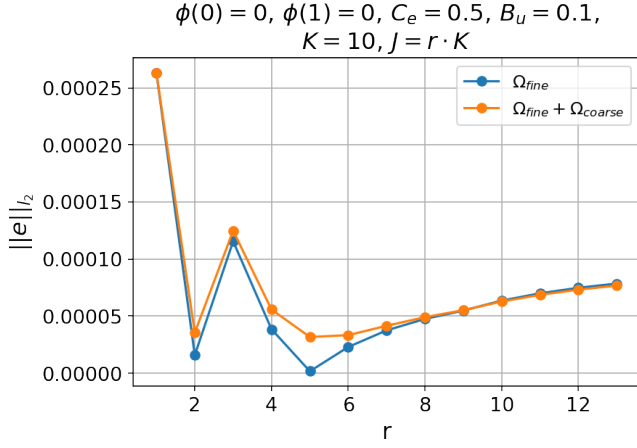


Figure 7: $\|e\|_{l_2}$ as compared to the analytic solution (10) for a constant B_u evaluated for BVP (9) with $a = b = 0$, varying $r = H/h$.

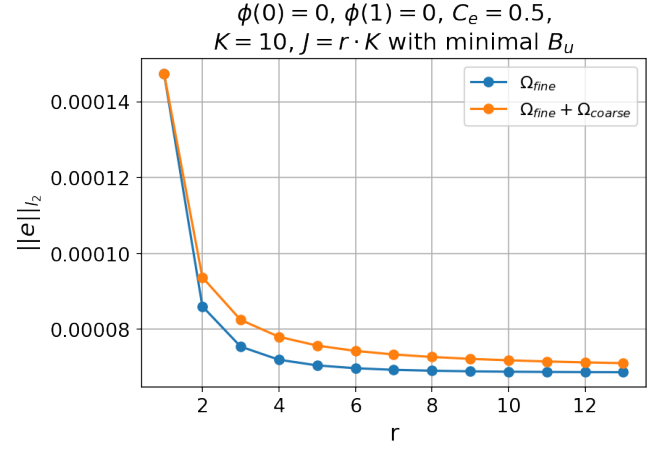


Figure 8: $\|e\|_{l_2}$ as compared to the analytic solution (10) for $B_u = B_u^{min}$ evaluated for BVP (9) with $a = b = 0$, varying $r = H/h$.

this time with dynamically varied $B_u = B_u^{min}$ (figure 8). Now we observe a smooth decrease of the error as we increase the